Control Engineering Practice 119 (2022) 104973

Contents lists available at ScienceDirect

Control Engineering Practice

journal homepage: www.elsevier.com/locate/conengprac

Optimal operation of an ice-tank for a supermarket refrigeration system ☆

Niclas Brok [a,*], Torben Green [b], Christian Heerup [c], Shmuel S. Oren [d], Henrik Madsen [a]

[a] Department of Applied Mathematics and Computer Science at the Technical University of Denmark, Denmark
[b] Danfoss A/S., Denmark
[c] Danish Technological Institute, Denmark
[d] Department of Industrial Engineering and Operations Research at the University of California at Berkeley, United States of America

ARTICLE INFO

Keywords:
Optimal control
Refrigeration system
Ice storage
Electricity markets
Optimal switching times
Optimization
Stochastic differential equations

ABSTRACT

The increasing proportion of renewable energy sources in power grids leads to challenges concerning balancing production and consumption. One solution to this grid challenge is to utilize demand-side flexibility. To use the full potential of demand-side flexibility, dynamical models and optimal control methods must be used. This paper demonstrates how demand-side flexibility can be enabled for a refrigeration system using an add-on ice-tank module to actively curtail the refrigeration system and thereby leveraging time-varying power prices. The operation of the ice-tank is the solution to an optimal control problem that minimize the integrated electricity costs. This optimal control problem is solved numerically and the performance of the strategy is successfully tested in a real experiment where cost-savings of approximately 20% are observed (compared to not having an ice-tank available). The proposed optimal control strategy is tested in real-life experiments spanning over 24 h. The dynamical relation between the operation of the ice-tank and the power consumption (the compressor capacity) is modelled using stochastic differential equations. This differential equation model is calibrated on 13 h of training data using the continuous–discrete Kalman filter and the maximum likelihood framework.

1. Introduction

Recently, Denmark agreed on its first ever Climate Bill, committing to reduce greenhouse gas emissions by more than 70% by 2030 compared to the Danish emission levels in 1990 (Denmark, 2019). This will increase the need for renewable energy sources and efficient integration will increase the need for demand-side flexibility (Ueckerdt, Brecha, & Luderer, 2015). This paper demonstrates a real example of short-term demand-side flexibility by curtailment of the power consumption of a refrigeration system using an add-on ice-tank module. The ice-tank operation (i.e when the ice-tank curtails the refrigeration system) is the solution to an optimal control problem which minimize the integrated power costs. The refrigeration system is located at the Danfoss test facility in Nordborg, Denmark. This refrigeration system resembles a small retail or supermarket refrigeration system.

Denmark has approximately 4500 supermarkets distributed across the country. These supermarkets consume more than 550,000 MWh per year, which constitutes about 2% of the annual Danish power consumption (Hovgaard, Larsen and Jørgensen, 2011). The power consumption of supermarkets comes from e.g. electric heating, lighting, and cooling. The installed cooling capacity varies a lot between supermarkets but is typically in the range from 10 to 200 kW, depending on the size of the refrigeration system. The refrigerated goods in the refrigeration units can have a large thermal capacity, thereby enabling flexibility in the refrigeration system.

The literature contains a lot of work concerning online control and forecasting of supermarket refrigeration systems and their power consumption. In Hovgaard, Larsen, Skovrup and Jørgensen (2011), a continuous time model based on ordinary differential equations is introduced. This model is used in an economic model predictive control algorithm, where the total cost of the electricity consumption associated with the refrigeration system is minimized. This economic model predictive control algorithm is extended in Vinther et al. (2016) to also consider a balancing market to further reduce the operational cost of the refrigeration system. Similarly, Larsen, Thybo, and Rasmussen (2007) applies a model predictive control scheme to optimize the daily operation of a refrigeration system to reduce the power consumption. Glavan, Gradišar, Humar, and Vrančić (2018) uses a

☆ This work is partially funded by the CITIES project (Danish Innovation fund, Denmark. Grant DSF 1305-00027B) and the ELFORSK project ELIS, Denmark (project number 345-028). The work has partially been conducted during an external research stay with CITRIS at the University of California at Berkeley where Niclas Brok visited Shmuel S. Oren for 5 months. This external research stay has been partially funded by the Danish Minstry of Higher Science and Education, Denmark.

* Corresponding author.
E-mail address: nlbr@dtu.dk (N. Brok).

https://doi.org/10.1016/j.conengprac.2021.104973
Received 7 August 2020; Received in revised form 17 August 2021; Accepted 19 October 2021
Available online xxxx
0967-0661/

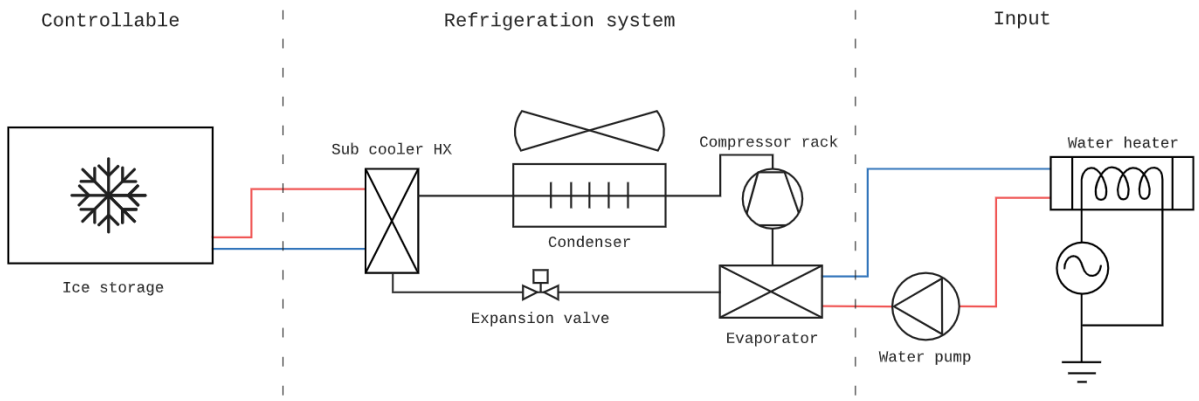

Fig. 1. This figure shows an overview of the total refrigeration system used to test the performance of optimally controlling an ice-tank.

control strategy to use the demand-side flexibility in a refrigeration system to reduce the peak power demand and thereby reduce the electricity costs. Hovgaard, Larsen, Edlund, and Jørgensen (2012) considers the value of operating and offering flexibility of refrigeration systems. Rasmussen et al. (2016) introduces a discrete time model for load forecasting a supermarket refrigeration system. This model distinguishes between supermarket opening hours and closing hours to improve longer horizon forecasts. Altwies and Reindl (2002) and Goli, McKane, and Olsen (2011) discusses the potential of demand-side flexibility for refrigerated warehouses. In Heerup and Green (2014), a rule-based control method is used (charging the ice-storage during the night, and melting during daytime) to investigate whether ice-storage is financially feasible for retail CO2-based refrigeration systems. Barzin, Chen, Young, and Farid (2015) presents a simulation study based on electricity tariffs from New Zealand, where a price-based control strategy is used to optimize a thermal storage for a freezer. Murphy, O'Mahony, and Upton (2015) compares different control systems to optimize ice-storage for food refrigeration. In Dowling, Kumar, and Zavala (2017), a financial analysis of actively operating a battery under Californian market conditions is investigated. This paper demonstrates that, under perfect information conditions, optimally managing the battery and bidding in multiple electricity markets can create much larger revenues compared to participation only in a traditional spot market.

This paper uses continuous–discrete models to estimate a dynamical model of the total refrigeration system. This continuous–discrete models have been used for a wide range of modelling and control related applications in the literature: for diabetes modelling in Duun-Henriksen et al. (2013), for modelling of heat dynamics of a building in Bacher and Madsen (2011) and Kristensen, Madsen, and Jørgensen (2004), and for modelling and control of wastewater aeration in Brok, Munk-Nielsen, Madsen, and Stentoft (2019, 2020).

1.1. Key contributions and paper organization

The existing literature presents few real experiments which test the proposed strategies. In the context of the reviewed literature, this work answers the following research questions:

- How can continuous–discrete stochastic systems be used to model the joint refrigeration and ice-tank system?
- What are the cost-savings potential of optimally operating the joint refrigeration and ice-tank system?

To answer these research questions, an optimal control problem is formulated; this optimization problem is based on a stochastic differential equation model which is calibrated to a training data-set with discrete observations. Using this differential equation model, the optimal control problem yields a numerical algorithm that optimally curtails a small retail refrigeration system using the add-on ice-tank module. This model formulation has two main advantages: (1) the estimation process is independent of the sampling rate and can easily manage irregular sampled observations, and (2) the estimation process is based on a maximum likelihood framework. This is in contrast to discrete-time methods used in the existing literature where the model parameters are dependent on the sampling time.

The performance of the optimal control algorithm is tested in a real physical experiment where cost-savings of approximately 20% are observed (compared to not having an ice-tank available).

This paper is structured as follows: first, the joint refrigeration and ice-tank is introduced. This section also contains an example of operation of this joint system. The second section describes how a continuous–discrete stochastic model (formulated using a stochastic differential equation (SDE) with discrete observations) can be calibrated to a data-set. This section also presents a one-state model of the compressor capacity of the joint refrigeration and ice-tank system. The third section introduces the Nordic power market. The fourth section defines the optimal control algorithm. The fifth section presents the results of operating the ice-tank in a real experiment using the optimal control algorithm. The paper concludes with a discussion of the results, a future outlook for the proposed optimal control algorithm and a brief summary.

2. The refrigeration system

The test refrigeration system is located at a Danfoss test facility in Nordborg, Denmark. The system compressors have a rated power consumption of approximately 12.4 kW. The power consumption of the compressors is the only source of power consumption considered in this paper. At the Danfoss test facility it is possible to simulate an outdoor temperature. In this study, this temperature is fixed at an average of approximately 35 °C. This corresponds to a very warm Danish Summer day. The ice-tank used is an `Ice Bear 40`, manufactured by `Ice Energy`. It is possible to alternate the mode of this ice-tank using an API service. The ice-tank can be in the following three modes:

- `CHARGE`, in this mode the ice-tank builds up the ice-storage. The rated power consumption in this mode is approximately 3 kW.
- `IDLE`, in this mode the ice-tank does nothing. This mode has a small power consumption (approximately 9 W), and due to imperfect insulation there is also a small thermal loss (i.e. a small reduction of the ice-storage).
- `MELT`, in this mode the ice-tank melts the ice-storage and starts curtailing the power consumption of the refrigeration system. In this mode the ice-tank has a small power consumption (approximately 250 W).

The latency of the API service is in the order of magnitude of 1–2 min due to communication via a third party server from which the ice-tank pulls data and commands.

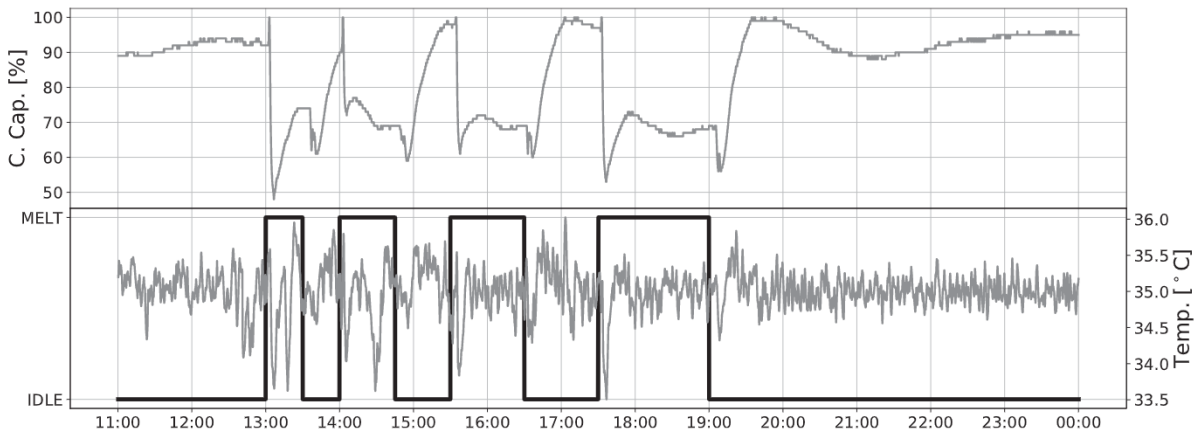

Fig. 2. This figure shows the results of the initial ice-tank test. This data is used to calibrate the dynamical model which will be used in the optimal control problem defined later. The top plot shows the compressor capacity (measured in %) and the bottom plot shows the ice-tank regime and the outdoor temperature (measured in °C). The refrigeration system is sampled every six seconds.

Fig. 1 shows a schematic overview of the test setup. The left part of this illustration is the ice-tank, which is the controllable component of the total refrigeration system. The middle part is the existing refrigeration system, which will be considered as a non-controllable system. The ice-tank is connected to the refrigeration system via a sub-cooler. To artificially emulate an outdoor temperature, a water heater is connected to the refrigeration system's evaporator via a water pump. This water heater can be used to emulate a fixed outdoor air temperature and this has been done in this study.

Note: Tests with lower outdoor temperatures have also been done. However, these results will not be presented, although they will briefly be discussed later.

In the next section, a dynamical model of the dynamical interplay between the refrigeration system and the ice-tank is defined. To calibrate this model to the actual system under consideration, a test data-set has to be generated. To generate this data-set, the ice-tank is alternated through four melt-cycles:

- A cycle with 30 min of `MELT` followed by 30 min of `IDLE` (from `13:00` until `14:00`).
- A cycle with 45 min of `MELT` followed by 45 min of `IDLE` (from `14:00` until `15:30`).
- A cycle with 60 min of `MELT` followed by 60 min of `IDLE` (from `15:30` until `17:30`).
- The final melt cycle is 90 min long and begins from `17:30`. When this cycle ends, the ice-tank remains in the `IDLE` mode.

These cycles – together with the compressor capacity and the outdoor temperature – can be seen in Fig. 2. The effect of the ice-tank switching to and from the `MELT` regime is clearly observed. From Fig. 2 it is also seen that the simulated outdoor temperature also exhibits larger oscillations when a mode-change of the ice-tank is implemented. This is due to the change in the work-load of the refrigeration compressors. This initial cycling of the system only ran for 13 h due to a busy schedule at the Danfoss test facility.

In the next section, a method for calibrating a dynamical model (in terms of an SDE) to the test data-set shown in Fig. 2 will be presented.

3. Modelling using SDEs

Modelling physical systems using SDEs provides a natural method to represent the phenomenon as it evolves in continuous time. A priori knowledge about the system can be included, and the estimated parameters do not depend on the sampling time (unlike for discrete-time models). The representation of noise in continuous time also allows for a parsimonious representation that is independent of the sampling time.

This section describes how to use SDEs to model the dynamical interaction between the refrigeration system and the ice-tank. This joint system can be considered as a continuous–discrete stochastic system (Jazwinski, 1970). The model used in this paper is an SDE with discretely sampled observations defined according to

$$\mathrm{d}x(t) = f(x(t), u(t); p)\mathrm{d}t + g(x(t), u(t); p)\mathrm{d}\omega(t), \tag{1a}$$

$$y_k = h(x(t_k); p) + v_k, \tag{1b}$$

where x, u, y and p are the states, inputs, observations and time-invariant parameters. $v_k \sim N_{\text{iid}}(0, R_k)$ is the measurement noise and ω is a standard Brownian motion. Brownian motion is defined by its independent increments which satisfy that for each $s, t \in \mathbb{R}$, $\omega(t)-\omega(s)$ is normally distributed with zero mean and covariance $I(t-s)$; i.e. $\mathrm{d}\omega(t) \sim N_{\text{iid}}(0, I\mathrm{d}t)$. $f : \mathbb{R}^{n_x}\times\mathbb{R}^{n_u}\to\mathbb{R}^{n_x}$ is often referred to as the drift function, while $g : \mathbb{R}^{n_x}\times\mathbb{R}^{n_u}\to\mathbb{R}^{n_x}\times\mathbb{R}^{n_\omega}$ is called the diffusion function. In this notation, n_x, n_u and n_ω denote the number of states, inputs and Brownian motions, respectively. The stochastic model defined in (1) is also referred to as a continuous–discrete stochastic state–space model where the dynamics are defined according to an SDE with discrete observations. The values, $\{t_k\}_{k=0}^{M}$, denote the sampling times of the continuous–discrete system.

For the joint system consisting of the ice-tank and the refrigeration system, the state of the system, x, will be the compressor capacity and the input, u, will be the ice-tank mode (i.e. a binary switch, modelling if the ice-tank is in `IDLE` or `MELT` mode). The parameters, p, will parameterize the dynamical relations between the ice-tank mode and the compressor capacity. The definitions of the functionals, f, g and h, and the unknown parameters, p, will be defined after the introduction of the continuous–discrete extended Kalman filter (CDEKF) and the associated maximum likelihood (ML) method. For further reading concerning the CDEKF and ML methods for SDEs, the authors refer to Jazwinski (1970) and Oksendal (2013).

3.1. Estimating parameters embedded in SDEs

The method presented next uses the CDEKF to evaluate the likelihood for a batch of data (Kristensen et al., 2004). The CDEKF is based on two schemes: a prediction scheme and an updating scheme. These schemes are briefly introduced in the following. $\hat{x}_{k-1}$ and $\hat{P}_{k-1}$ will denote the mean and covariance predictions of the state, x, while $\hat{x}_{k-1|k-1}$ and $\hat{P}_{k-1|k-1}$ will denote the mean and covariance filtered estimates of x (or reconstructions).

3.1.1. The prediction scheme

Given the initial conditions

$$\hat{x}_{k-1}(t_{k-1}) = \hat{x}_{k-1|k-1}, \quad \hat{P}_{k-1}(t_{k-1}) = \hat{P}_{k-1|k-1}, \tag{2}$$

the state and covariance are predicted by solving the system of ordinary differential equations (ODEs) given by

$$\dot{\hat{x}}_{k-1}(t) = f(\hat{x}_{k-1}(t), u(t); p), \tag{3a}$$

$$\dot{\hat{P}}_{k-1}(t) = A(t)\hat{P}_{k-1}(t) + \hat{P}_{k-1}(t)A(t)' + G(t)G(t)', \tag{3b}$$

where

$$A(t) = \frac{\partial f}{\partial x}(\hat{x}_{k-1}(t), u(t); p), \quad G(t) = g(\hat{x}_{k-1}(t), u(t); p).$$

The one-step predictions of the mean and covariance of the states are obtained as the solution of (2)–(3) at the new sample point, t_k. Consequently, the predictions of the mean and covariance are

$$\hat{x}_{k|k-1} = \hat{x}_{k-1}(t_k), \quad \hat{P}_{k|k-1} = \hat{P}_{k-1}(t_k). \tag{4}$$

3.1.2. The updating scheme

The literature contains many methods for the updating scheme in extended Kalman filter algorithms. They all compute the innovation by

$$e_k = y_k - h(\hat{x}_{k|k-1}), \tag{5}$$

the Kalman filter gain, K_k, by

$$C_k = \frac{\partial h}{\partial x}(\hat{x}_{k|k-1}), \tag{6a}$$

$$R_{k|k-1} = C_k \hat{P}_{k|k-1} C_k' + R_k, \tag{6b}$$

$$K_k = \hat{P}_{k|k-1} C_k' R_{k|k-1}^{-1}, \tag{6c}$$

and the filtered state estimate, $\hat{x}_{k|k}$, by

$$\hat{x}_{k|k} = \hat{x}_{k|k-1} + K_k e_k. \tag{7}$$

The key difference is how they compute the filtered covariance, $P_{k|k}$. Two standard updating schemes for the covariance are

$$\hat{P}_{k|k} = \left(I - K_k C_k\right) \hat{P}_{k|k-1} \tag{8a}$$

$$= \hat{P}_{k|k-1} - K_k R_{k|k-1} K_k'. \tag{8b}$$

Numerical implementations based on either (8a) or (8b) may give rise to bad performance and even divergence, as the *numerically* computed values are not guaranteed to be both positive (semi-)definite and symmetric. The Joseph stabilization form

$$\hat{P}_{k|k} = \left(I - K_k C_k\right) \hat{P}_{k|k-1} \left(I - K_k C_k\right)' + K_k R_k K_k'. \tag{9}$$

for updating the filtered covariance estimate guarantees that the numerical value of $P_{k|k}$ is symmetric positive (semi-)definite.

3.1.3. Maximum likelihood estimation

Using the one-step prediction errors, from the prediction and updating schemes, the likelihood of the model parameters given the discretely sampled observations can be computed; the parameters that maximize this likelihood computation will be used as the model parameters for the model used in the optimal control problem. In this section, this likelihood calculation is introduced.

Let $\{y_j\}_{j=1}^M$ denote M observations relating to the sample points $\{t_j\}_{j=1}^M$ in (1b). Define the information accumulated up until the kth sample point as $\mathcal{Y}_k = \{y_j\}_{j=1}^k$. Then the likelihood function, $\mathcal{L}$, can be defined as

$$\mathcal{L}\left(p \mid \mathcal{Y}_M\right) \propto \phi\left(\mathcal{Y}_M \mid p\right), \tag{10}$$

where ϕ is the joint density function of the observations, $\mathcal{Y}_M$. Using the definition of conditional probabilities, the right hand side can be decomposed into

$$\phi\left(\mathcal{Y}_M \mid p\right) = \prod_{k=1}^{M} \phi\left(y_k \mid \mathcal{Y}_{k-1}, p\right), \tag{11}$$

Table 1
Estimated parameters of the SDE.

Parameter	Description	Value	Unit
p_1	MELT rate	0.00183	%/s
p_2	MELT asymptotic level	66.92400	%
p_3	IDLE rate	0.00085	%/s
p_4	IDLE asymptotic level	94.89100	%
p_5	Diffusion coefficient	0.28130	–
p_6	Observation variance	1.96580	–

such that the log-likelihood function can be expressed by

$$\log\left(\mathcal{L}\left(p \mid \mathcal{Y}_M\right)\right) = \sum_{k=1}^{M} \log\left(\phi\left(y_k \mid \mathcal{Y}_{k-1}, p\right)\right). \tag{12}$$

Consequently, the ML parameter estimates, p_{ML}, are given by

$$\begin{aligned} p_{\mathrm{ML}} &\in \arg\max_{p \in \mathbb{R}^{n_p}} \log\left(\mathcal{L}(p \mid \mathcal{Y}_M)\right) \\ &= \arg\max_{p \in \mathbb{R}^{n_p}} \sum_{k=1}^{M} \log(\phi(y_k \mid \mathcal{Y}_{k-1}, p)), \end{aligned} \tag{13}$$

where n_p denotes the number of parameters. The SDE in (1a) is driven by a Brownian motion, and since the increments of a Brownian motion are Gaussian, it is reasonable to assume that, under some regularity conditions, the conditional densities in (11) can be well approximated by Gaussian densities

$$\phi(y_k \mid \mathcal{Y}_{k-1}, p) = \frac{\exp\left(-\frac{1}{2} e_k' R_{k|k-1}^{-1} e_k\right)}{\sqrt{\det(R_{k|k-1})(2\pi)^{n_y}}}, \tag{14}$$

where n_y is the number of output variables.

3.2. Estimating the refrigeration system model

The drift function, f, will be parameterized according to

$$f(x(t), u(t); p) = \begin{cases} p_1(p_2 - x(t)), & t \in \texttt{MELT} \\ p_3(p_4 - x(t)), & t \in \texttt{IDLE}. \end{cases} \tag{15}$$

By defining the input function, u, as

$$u(t) = \left(\mathbb{1}(t \in \texttt{MELT}), \mathbb{1}(t \in \texttt{IDLE})\right)'. \tag{16}$$

where

$$\mathbb{1}(t \in I) = \begin{cases} 1, & t \in I \\ 0, & t \notin I \end{cases}, \tag{17}$$

the drift function can be defined according to

$$\begin{aligned} f(x(t), u(t); p) = {} & u_1(t) p_1 (p_2 - x(t)) \\ & + u_2(t) p_3 (p_4 - x(t)). \end{aligned} \tag{18}$$

It is assumed that the incremental covariances are constant, and hence the diffusion function, g, is defined as a positive parameter, p_5. g is parameterized as

$$g(x(t), u(t); p) = p_5. \tag{19}$$

The compressor capacity is observed directly. The function h is therefore defined as

$$h(x(t_k); p) = x(t_k). \tag{20}$$

The variance of the uncertainty of the observations is also defined as a positive parameter

$$R_k = p_6, \tag{21}$$

which means that the variance is assumed to be time-invariant. The parameters are estimated using CTSM-R (Juhl, Møller, & Madsen, 2016) and the parameter estimates are listed in Table 1.

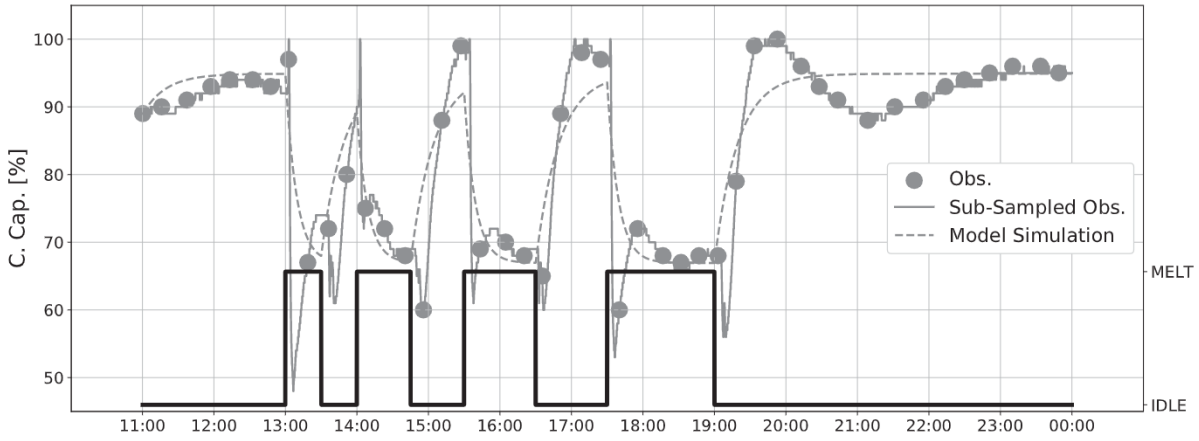

Fig. 3. This figure shows the results of a full-horizon simulation using the first-order model. The dashed grey line is the model predictions, the grey dots are the sub-sampled observations, the solid grey line is the high-frequent observations and the solid black line is the ice-tank input.

The data sampled from the Danfoss test system is sampled at a very high frequency (around every six seconds) compared to the time-constants of the dynamical system. The observations have been sub-sampled such that the observations of the data-set used within `CTSM-R` are sampled every 15 min (one observation every 15 min). In Fig. 3, a full-horizon simulation using the estimated first-order, two-regime model introduced above, is shown. The solid black line represents the schedule of the switching function, u, the filled grey dots are the sub-sampled observations, the solid grey line represents the observations of the full data-set and the dashed grey line is the compressor capacity forecast given by the model introduced above. The forecast is not updated for each observation and is therefore a full horizon forecast (or simulation); the dashed grey line is the solution to the prediction scheme of the CDEKF.

4. The nordic electricity market

In Northern Europe, electricity is traded in a common market called Nord Pool, which consists of 15 interconnected price areas. The market trading with the largest volume is called the day-ahead market. Here, electricity is bought and sold for the upcoming day and this market sets the spot price. When the day-ahead market closes, the intra-day market opens. In this market, electricity can be traded until 45 min prior to the operating hour.

One of the primary challenges when operating transmission systems is to guarantee grid stability. The Nordic Transmission System Operators (TSOs) have many methods for dealing with this challenge; one of them being a common balancing market (Energinet, 2017). In the balancing market, market participants have the option to make a bid that defines how much a participant is willing to change their production or consumption schedule in a given operating hour. The balancing market also closes 45 min prior to the operating hour. Hence, when approaching the operating hour, the TSO has the possibility to activate balancing bids ahead of time and thereby reduce the risk of imbalances. Three scenarios can take place in the balancing market:

- (↑) If the imbalance is negative, there is a deficit of electricity in the price area, and hence an increase in power production or a decrease in power consumption is needed. This is called *up* regulation.
- (↓) If the imbalance is positive, there is a surplus of electricity in the price, and hence a decrease in power production or an increase power consumption is needed. This is called *down* regulation.
- (−) If the imbalance is too small or the duration is too short, the imbalance is not offered in the balancing market.

In a situation with up regulation, electricity is sold, while in the situation with down regulation, electricity is bought. The structure of the balancing market requires that the up regulation price is greater than the day-ahead price, while the down regulation price is lower than the day-ahead price. In the price area DK1, a large share of the total power production is generated by wind turbines. In Parbo (2014) it is suggested that approximately 65% of the total imbalances in DK1 are due to forecast errors of wind power production.

In the optimal control problem defined later, it is assumed that the combined refrigeration and ice-tank system is a price-taker of the spot price. The potential of also participating in the balancing market is not considered. However, it should be emphasized that the savings shown later in this paper should be regarded as a lower bound of the savings one can expect from e.g. also participating in a balancing market.

5. The optimization problem

In this section, the optimization problem for the optimal switching times is defined. The system dynamics embedded into the optimization problem formulation are ordinary differential equations (ODEs) defined by the drift function in (15) with the parameters, p, listed in Table 1.

5.1. Optimal control by optimal switching times

The drift function, f, in (15) is a regime-type function defined by a set of switching times. Define the set of switching times $\tau = \left\{\tau_{i,\texttt{MELT}}, \tau_{i,\texttt{IDLE}}\right\}_{i=0}^{N}$ for which the structure

$$\tau_{i,\texttt{MELT}} \leq \tau_{i+1,\texttt{IDLE}}, \tag{22a}$$

$$\tau_{i,\texttt{IDLE}} \leq \tau_{i,\texttt{MELT}}, \tag{22b}$$

is imposed. The variables $\left\{\tau_{i,\texttt{MELT}}\right\}_{i=0}^{N}$ denote the temporal switches for when the ice-tank curtails the refrigeration system, and hence de-loads the system, and the variables $\left\{\tau_{i,\texttt{IDLE}}\right\}_{i=0}^{N}$ denote the temporal switches for when the ice-tank stops curtailing the refrigeration system and the system returns to normal operation. The number of switching times, N, is a design parameter of the optimal control problem; different values of N will lead to different control strategies. In this paper $N = 5$ is chosen.

Using these temporal switches, f can be defined according to the temporal decomposition given by

$$\begin{aligned} f(x(t), t; p) = &\sum_{i=0}^{N-1} \mathbb{1}\left(t \in \boldsymbol{I}_{i,\texttt{MELT}}\right) f_{\texttt{MELT}}(x(t); p) \\ &+ \sum_{i=0}^{N} \mathbb{1}\left(t \in \boldsymbol{I}_{i,\texttt{IDLE}}\right) f_{\texttt{IDLE}}(x(t); p), \end{aligned} \tag{23}$$

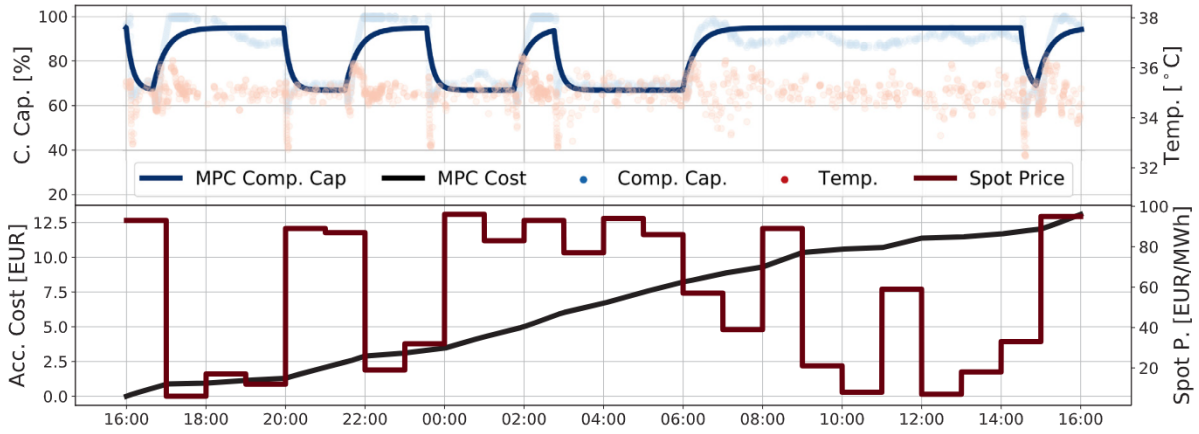

Fig. 4. This figure shows the online results of actually implementing the optimal switching times. The top plot shows the predicted compressor capacity (left axis) together with the emulated outdoor temperature (right axis). The bottom plot shows the accumulated cost (left axis) and the used spot price (right axis).

where the intervals $I_{i,\mathrm{MELT}}$ and $I_{i,\mathrm{IDLE}}$ are defined according to

$$I_{i,\mathrm{MELT}} = [\tau_{i,\mathrm{MELT}}, \tau_{i+1,\mathrm{IDLE}}[\tag{24a}$$

$$I_{i,\mathrm{IDLE}} = [\tau_{i,\mathrm{IDLE}}, \tau_{i,\mathrm{MELT}}[, \tag{24b}$$

and the functionals f_{MELT} and f_{IDLE} according to

$$f_{\mathrm{MELT}}(x;p) = p_1(p_2 - x) \tag{25a}$$

$$f_{\mathrm{IDLE}}(x;p) = p_3(p_4 - x). \tag{25b}$$

The convention $\tau_{0,\mathrm{IDLE}} = 0$ and $\tau_{N,\mathrm{MELT}} = T$ will be used, for which the parameter $T > 0$ will denote the simulation horizon for the optimal control problem defined later in this section.

Let x represent the only state of the system. This state models the compressor capacity. Besides the electricity cost of running the compressors, there is also a cost associated with operating the ice-tank in the two regimes. Let $c(x(t), t)$ denote the total cost of operating the combined system consisting of the refrigeration system and the ice-tank at time t with a compressor capacity of the refrigeration system of $x(t)$. The total cost rate c is then given by

$$\begin{aligned} c(x(t), t; \tau) &= q(t) \\ &\times \left(kx(t) + k_{\mathrm{MELT}} \sum_{i=0}^{N-1} \mathbb{1}\left(t \in I_{i,\mathrm{MELT}}\right) \right. \\ &\left. + k_{\mathrm{IDLE}} \sum_{i=0}^{N} \mathbb{1}\left(t \in I_{i,\mathrm{IDLE}}\right) \right), \end{aligned} \tag{26}$$

where $q(t)$ represents the electricity cost at time t, k is the rated capacity of the compressor, k_{MELT} is the electricity consumption of the ice-tank cost when it is curtailing the refrigeration system, and k_{IDLE} is the electricity consumption of the ice-tank when it is idle. Integrating this instantaneous total cost rate, $c(x(t), t)$, yields the accumulated total cost

$$J(x, \tau) = \int_0^T c(x(t), t; \tau)\mathrm{d}t. \tag{27}$$

This functional will be the objective function of the optimal control problem defined next.

Using the definitions and variables defined above, the optimal control problem is defined according to

$$\min_{x,\tau} \left\{ J(x, \tau) = \int_0^T c(x(t), t; \tau)\mathrm{d}t \right\}, \tag{28a}$$

s.t.

$$\tau \in \mathcal{T}, \tag{28b}$$

$$\dot{x} = f(x; p, \tau), \quad \text{in } [0, T], \tag{28c}$$

$$x(0) = x_0, \tag{28d}$$

where the set $\mathcal{T}$ defines the temporal structure given in (22) together with the temporal budget constraint given by

$$\sum_{i=0}^{N} \left(\tau_{i+1,\mathrm{IDLE}} - \tau_{i,\mathrm{MELT}}\right) \leq \overline{\tau}. \tag{29}$$

This budget constraint is due to the fact that the ice-tank only has a finite amount of ice available and the constraint will also ensure that the trivial case, where the ice-tank is only curtailing the refrigeration system, becomes infeasible (assuming that $\overline{\tau}$ is chosen properly). The constraint in (29) models the maximum allowed time of curtailment. In this paper, this budget parameter is defined as $\overline{\tau} = 8$ h.

Note: An extra argument to the functions c and f in (28a) and (28c) has been included to indicate the dependence of the switching times, τ.

5.2. Analytical gradient expression

To enable efficient numerical solution of the optimal control problem (28), gradient information has to be made available to the optimization algorithm. The Jacobians of the temporal constraints in (28b) are trivial, since these constraints are all linear. Hence, the only derivatives that are non-trivial, are the derivatives that relate to the objective function (28a). The gradient of the objective function contains the elements

$$\frac{\partial J}{\partial \tau_{j,\mathrm{MELT}}}(x, \tau) \quad \text{and} \quad \frac{\partial J}{\partial \tau_{j,\mathrm{IDLE}}}(x, \tau). \tag{30}$$

Analytical expressions of these will be derived in the following. These expressions are based on derivations and results from Axelsson, Egerstedt, Wardi, and Vachtsevanos (2005).

First, derivatives with respect to $\tau_{k,\mathrm{MELT}}$ are considered. Inserting the definition of J yields

$$\frac{\partial J}{\partial \tau_{j,\mathrm{MELT}}}(x, \tau) = \frac{\partial}{\partial \tau_{j,\mathrm{MELT}}} \int_0^T c(x(t), t; \tau)\mathrm{d}t, \tag{31}$$

Using the definition of the indicator function of the temporal decomposition, the integral in (31) can be defined as

$$\begin{aligned} \int_0^T c(x(t), t; \tau)\mathrm{d}t &= \int_0^T kq(t)x(t)\mathrm{d}t \\ &+ k_{\mathrm{MELT}} \sum_{i=0}^{N-1} \int_{\tau_{i,\mathrm{MELT}}}^{\tau_{i+1,\mathrm{IDLE}}} q(t)\mathrm{d}t \\ &+ k_{\mathrm{IDLE}} \sum_{i=0}^{N} \int_{\tau_{i,\mathrm{IDLE}}}^{\tau_{i,\mathrm{MELT}}} q(t)\mathrm{d}t. \end{aligned} \tag{32}$$

Using (32), the derivatives with respect to $\tau_{k,\texttt{MELT}}$ simplify into

$$\frac{\partial J}{\partial \tau_{j,\texttt{MELT}}}(x,\tau) = \frac{\partial}{\partial \tau_{j,\texttt{MELT}}} \int_0^T kq(t)x(t)\mathrm{d}t + \left(k_{\texttt{IDLE}} - k_{\texttt{MELT}}\right) q\left(\tau_{j,\texttt{MELT}}\right), \tag{33}$$

where the first term can be computed using the adjoint states (or co-states) for the optimal control problem (Axelsson et al., 2005). The co-states (to be denoted by λ) satisfy the dynamical equations

$$\begin{aligned} \dot{\lambda} &= -\frac{\partial f}{\partial x}(x;p,\tau)'\lambda - \frac{\partial c}{\partial x}(x,\cdot;\tau)', \quad \text{in } [0,T] \\ \lambda(T) &= 0. \end{aligned} \tag{34}$$

Using the results from Axelsson et al. (2005), the derivatives with respect to $\tau_{k,\texttt{MELT}}$ can be computed from

$$\begin{aligned} &\frac{\partial J}{\partial \tau_{j,\texttt{MELT}}}(x,\tau) = \\ &\lambda(\tau_{j,\texttt{MELT}})'\left(f_{\texttt{IDLE}}(x(\tau_{j,\texttt{MELT}});p) - f_{\texttt{MELT}}(x(\tau_{j,\texttt{MELT}});p)\right) \\ &\quad + \left(k_{\texttt{IDLE}} - k_{\texttt{MELT}}\right) q\left(\tau_{j,\texttt{MELT}}\right). \end{aligned} \tag{35}$$

The result in (35) is not valid for $\tau_{N,\texttt{MELT}}$. However, this variable is by convention fixed ($\tau_{N,\texttt{MELT}} = T$) and will not be subject to the optimization.

Following the same steps as above, a similar result can be derived for the derivatives of the objective function (28a) with respect to $\tau_{j,\texttt{IDLE}}$. The derivatives with respect to these variables can be computed from

$$\begin{aligned} &\frac{\partial J}{\partial \tau_{j,\texttt{IDLE}}}(x,\tau) = \\ &\lambda(\tau_{j,\texttt{IDLE}})'\left(f_{\texttt{MELT}}(x(\tau_{j,\texttt{IDLE}});p) - f_{\texttt{IDLE}}(x(\tau_{j,\texttt{IDLE}});p)\right) \\ &\quad + \left(k_{\texttt{MELT}} - k_{\texttt{IDLE}}\right) q\left(\tau_{j,\texttt{IDLE}}\right). \end{aligned} \tag{36}$$

The result in (36) is not valid for $\tau_{0,\texttt{IDLE}}$. However, this variable is by convention fixed ($\tau_{0,\texttt{IDLE}} = 0$) and will not be subject to the optimization.

Note: The implementation of the numerical solution of the optimal control problem (28) is done using a single-shooting formulation (Bock & Plitt, 1984; Diehl, Bock, Diedam, & Wieber, 2006). This means that the dynamical Eqs. (28c)–(28d) are solved internally of the implemented objective function. Thus, the only constraints needing to be implemented are the linear set of constraints defined by the temporal set of constraints in (28b).

5.3. Numerical implementation

The optimal control problem has been solved numerically in `python`. A single-shooting approach has been applied where the `solve_ivp` function from the `scipy` package has been used to solve the dynamical equations (the state and co-state equations). The Runge–Kutta 5(4) method with adaptive step size has been chosen as the numerical method (Dormand & Prince, 1980; Virtanen et al., 2019). The optimization algorithm used is a constrained trust-region method, which is available via the `minimize` function from the `scipy` package (Conn, Gould, & Toint, 2000).

6. Results

This section presents the results of implementing the optimal control algorithm defined in (28) for the total refrigeration system illustrated in Fig. 1. A single open-loop iteration of the optimal control problem is used to compute the optimal switching times. These switching times are used to operate the ice-tank for a period of 24 h (or one day). This implies that no feedback from the refrigeration system nor the ice-tank is used. The power prices are assumed to be known for the entire 24 h; this is a reasonable assumption as many retailers offer power prices which follows the spot price. The spot price is always known 12 h to 36 h ahead (depending on the time of day); hence, optimal control problem is run when there is at least 24 hourly power prices available (this is e.g. the case everyday at 4pm).

Table 2
Power consumption parameter.

Parameter	Description	Value	Unit
k	Rated compressor capacity	12.4	kW
$k_{\texttt{MELT}}$	MELT power consumption	250.0	W
$k_{\texttt{IDLE}}$	IDLE power consumption	9.0	W

The spot prices from a random day at Nord Pool have been used to generate a load input in terms of a price signal. The outdoor temperature is emulated using the water heater shown in Fig. 1, and this temperature is set to average around 35 °C such that the compressors of the existing refrigeration system would operate close to 100% when the ice-tank is in the `IDLE` mode. The temporal budget constraint parameter, $\overline{\tau}$, in (29) is defined such that the ice-tank can only be in the `MELT` mode for 8 h. It is assumed (in the financial analysis in Fig. 5) that the ice-tank has been charged with a zero cost. The values of the power consumption parameters k, $k_{\texttt{MELT}}$ and $k_{\texttt{IDLE}}$ used in the objective function of the optimal control problem are given in Table 2.

The optimal control algorithm optimally distributes five `MELT` periods throughout the 24 h of operation (starting at 4pm on the first day of testing). These cycles are distributed according to (rounded to nearest second):

1. `MELT` starts at `16:00:08` until `16:40:06`.
2. `MELT` starts at `19:57:34` until `21:29:45`.
3. `MELT` starts at `23:32:58` until `01:44:14`.
4. `MELT` starts at `02:45:01` until `05:58:25`.
5. `MELT` starts at `14:28:35` until `14:51:43`.

In Fig. 4, the results of operating the ice-tank using these optimal switching times are shown. The top plot shows the difference between the predicted compressor capacity (predicted by the SDE model) and the observed values. The bottom plot shows the spot prices used in the objective function together with predicted accumulated cost. In Fig. 5, the performance of operating the ice-tank is presented. The top plot shows the difference between actively operating the ice-tank and not having an ice-tank at all. The bottom plot shows the predicted savings and the realized savings. The realized savings are computed based on the observed compressor capacity values shown in the top plot of Fig. 4. From Figs. 4 and 5 the following observations are made:

- Fig. 4 shows that when the ice-tank is in `MELT`, the compressor capacity drops to approximately 67%. This corresponds to the parameter value of p_2 given in Table 1. From Fig. 4 it is also seen that the SDE model predicts too low compressor capacities when the ice-tank switches from `MELT` to `IDLE`. This is observed after the first three `MELT` cycles.
- From Fig. 4 it is observed that the emulated outdoor temperature exhibits a higher degree of variability when the ice-tank implements a mode change.
- Fig. 5 shows that there is some discrepancy between the predicted savings of operating the ice-tank and the realized savings. However, the predicted and realized savings are both in the order of approximately 20%. This discrepancy is expected, as the predicted savings are based on forecasts with a horizon of up to 24 h.

7. Discussion & future outlook

This section discusses some of the observed deficiencies observed for the SDE model used in the optimal control problem. A possible method for economical and efficient charging of the ice-tank is also discussed. In connection with this, it is also discussed how the optimal control

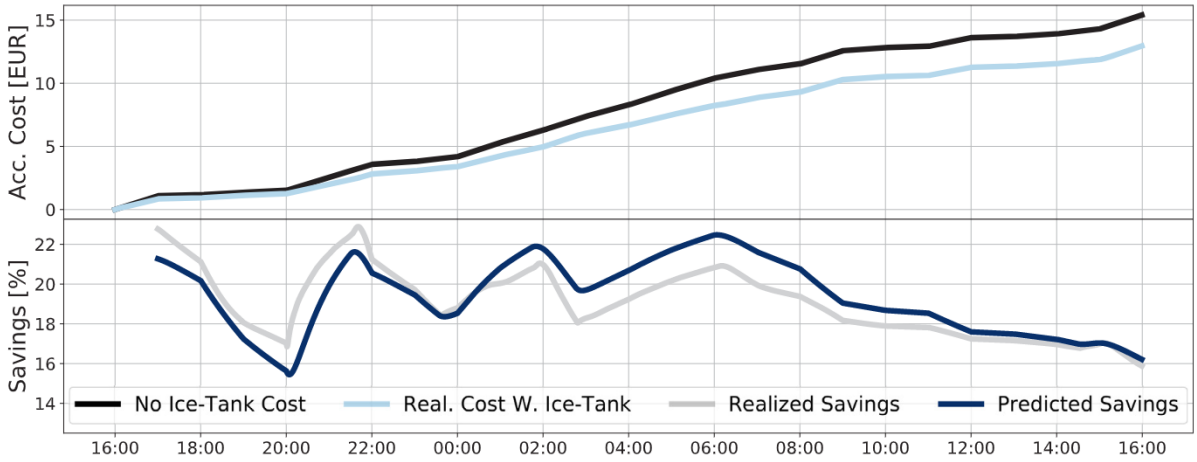

Fig. 5. This figure visualizes the effect of having the ice-tank installed. The top plot shows the accumulated cost of actively operating the ice-tank vs. not having the ice-tank. The bottom plot shows the relative savings of operating the ice-tank. The bottom plot shows how the predicted savings compare to the realized savings. It is assumed that the ice-tank has been charged with zero cost.

problem can be extended to include other load inputs than the spot price (e.g. CO2 emissions). Finally, the applicability of the ice-tank to other regions (than Scandinavia) and hence other electricity markets is discussed.

7.1. Extensions to the dynamical model

The dynamical model used in the optimal control problem in (28) has difficulties in explaining the transient dynamics observed in Figs. 2–4 when the ice-tank implements a mode change. One extension to the regime-based first-order model used to model the drift function (15) could be to include the outdoor temperature as a state in the SDE model such that the higher variability of the outdoor temperature might be explained by the model. A second extension could be to consider higher order models that better describe the dynamics observed after a mode change. The data presented in Figs. 2–4 suggest that a suitable model might be nonlinear, since the compressor capacity tends to drop both when the ice-tank switches from `IDLE` to `MELT` and from `MELT` to `IDLE`.

The SDE model used in this paper is estimated from data where the refrigeration system is measured under similar conditions. Hence, this model is indifferent to changing conditions such as e.g. opening and closing hours. In Rasmussen et al. (2016) it is shown that there is a clear difference in a supermarket's power consumption during opening and closing hours. Thus, in a real-life application the model has to be extended to accommodate such conditions. One solution to this might be to consider two different models for opening and closing hours respectively. Neither is the SDE model suitable under conditions where the outdoor temperature exhibits time-varying dynamics. Under such conditions, the model parameters, p, might all depend on the value of the outdoor temperature. A suitable extension to accommodate this might be (again) to include the outdoor temperature as a state in the SDE model.

Both of these extensions also address the importance of robustness of the controller. The method proposed in this paper has no state or parameter update step; however, to accommodate changing external conditions such as opening hours and outdoor temperatures, re-calibration of the dynamical model becomes very important. Using continuous–discrete stochastic systems, as the system introduced in (1), the re-calibration process can easily be included. These extensions will also influence the solution time of both the model calibration and the optimization algorithms. These solution times were observed to be insignificant in connection with the modelling and optimization done in this paper.

7.2. Optimal and sustainable charging of the ice-tank

In the calculations of the realized and predicted savings presented in Fig. 5, it is assumed that the ice-tank has been charged with zero cost. Naturally, under varying market conditions this will not always be feasible. However, one of the main advantages of using the ice-tank as the flexible component in the refrigeration system is that the only two constraints are the minimum and maximum capacities of the amount of ice that can be stored. If the refrigeration system itself had been subject to a control strategy as done in e.g. Hovgaard, Larsen, Skovrup et al. (2011), Larsen et al. (2007), Vinther et al. (2016) and Glavan et al. (2018), then the system would also be subject to hard constraints on e.g. the temperature of the display units. Hence, the ice-tank can be used to provide flexibility in a balancing market and thereby reduce the price of generating the stored ice. Furthermore, the optimal control problem can even be extended such that the ice-tank can be used to optimally distribute in which electricity market the power consumption is traded (day-ahead market, intra-day market, balancing market, etc.). It is expected that such formulations would heavily increase the observed savings, as the price differences become much larger. However, to take full advantage of this, a better model of the short-term dynamics is needed, together with a model that generalizes to varying exogenous conditions (e.g. the outdoor air temperature).

In the objective function used in the formulation of the optimal control problem in (28), only the cost associated with power consumption is considered. However, this objective function can easily be extended to also accommodate a cost associated with e.g. the CO2 emissions of power consumption. This type of combination of objectives for an electricity consumer is investigated in e.g. Junker et al. (2018).

7.3. Other electricity markets

The results presented in this paper rely heavily on the assumption of high outdoor temperatures such that the compressors yield a high power consumption. This is a constraining assumption for the applicability in Northern Europe, as the savings presented in Fig. 5 will only be feasible during the summer months. Experiments with lower temperatures have also been conducted. For these experiments, savings in the range from 5% to 10% are observed. Thus, lower outdoor temperatures will extend the payback period of the investments associated with the installation and maintenance of the ice-tank.

One region with higher average temperatures than Denmark and Scandinavia in general, is California. The Californian electricity market offers a variety of markets which might be economically beneficial to consumers who can deliver demand-side flexibility. In Dowling et al.

(2017) it is shown that participation in the Californian energy markets (day-ahead market, 15-min market and real-time market) and bidding for ancillary services (non-spinning reserves, spinning reserves and regulation) hugely increases the revenue potential of actively operating a battery. The paper shows that under perfect information conditions, the revenue generated from participation in the full-stack of electricity markets might be up to 600% larger than the revenue generated by only bidding in the day-ahead market. The ice-tank presented in this paper has many similarities to a battery. Thus, it is expected that larger savings (than shown in Fig. 5) are obtainable by actively bidding the flexibility generated by the ice-tank in multiple markets on different time-scales. However, this will require more accurate dynamical models of the interaction between the ice-tank and the refrigeration system.

8. Conclusion

The goal of this paper was to investigate the economic potential of actively operating an ice-tank connected to a refrigeration system using an optimal control algorithm. Based on the experiments presented in this paper, it is demonstrated that it is possible to lower the total electricity costs by approximately 20% with a temporal budget constraint for the ice-tank of 8 h. It is expected that larger savings are obtainable by actively bidding the flexibility generated by the ice-tank in multiple electricity markets. However, this will require more accurate dynamical models of the interaction between the ice-tank and the refrigeration system.

Declaration of competing interest

The authors declare that they have no known competing financial interests or personal relationships that could have appeared to influence the work reported in this paper.

References

Altwies, Joy E., & Reindl, Douglas T. (2002). Passive thermal energy storage in refrigerated warehouses. *International Journal of Refrigeration*, *25*(1), 149–157.

Axelsson, H., Egerstedt, M., Wardi, Y., & Vachtsevanos, G. (2005). Algorithm for switching-time optimization in hybrid dynamical systems. In *Proceedings of the 2005 IEEE international symposium on, mediterrean conference on control and automation intelligent control, 2005.* (pp. 256–261). IEEE.

Bacher, Peder, & Madsen, Henrik (2011). Identifying suitable models for the heat dynamics of buildings. *Energy and Buildings*, *43*(7), 1511–1522.

Barzin, Reza, Chen, John J. J., Young, Brent R., & Farid, Mohammed M. (2015). Peak load shifting with energy storage and price-based control system. *Energy*, *92*, 505–514.

Bock, Hans Georg, & Plitt, Karl-Josef (1984). A multiple shooting algorithm for direct solution of optimal control problems. *IFAC Proceedings Volumes*, *17*(2), 1603–1608.

Brok, Niclas Brabrand, Munk-Nielsen, Thomas, Madsen, Henrik, & Stentoft, Peter A. (2019). Flexible control of wastewater aeration for cost-efficient, sustainable treatment. *IFAC-PapersOnLine*, *52*(4), 494–499.

Brok, Niclas Brabrand, Munk-Nielsen, Thomas, Madsen, Henrik, & Stentoft, Peter A. (2020). Unlocking energy flexibility of municipal wastewater aeration using predictive control to exploit price differences in power markets. *Applied Energy*, *280*, Article 115965.

Conn, Andrew R., Gould, Nicholas I. M., & Toint, Ph. L. (2000). *Trust region methods, Vol. 1*. Siam.

(2019). *Denmark strikes deal to slash CO2 emissions by 70% in a decade*. Bloomberg.

Diehl, Moritz, Bock, Hans Georg, Diedam, Holger, & Wieber, P.-B. (2006). Fast direct multiple shooting algorithms for optimal robot control. In *Fast motions in biomechanics and robotics* (pp. 65–93). Springer.

Dormand, John R., & Prince, Peter J. (1980). A family of embedded Runge-Kutta formulae. *Journal of Computational and Applied Mathematics*, *6*(1), 19–26.

Dowling, Alexander W., Kumar, Ranjeet, & Zavala, Victor M. (2017). A multi-scale optimization framework for electricity market participation. *Applied Energy*, *190*, 147–164.

Duun-Henriksen, Anne Katrine, Schmidt, Signe, Røge, Rikke Meldgaard, Møller, Jonas Bech, Nørgaard, Kirsten, Jørgensen, John Bagterp, et al. (2013). Model identification using stochastic differential equation grey-box models in diabetes. *Journal of Diabetes Science and Technology*, *7*(2), 431–440.

Energinet, D. K. (2017). Regulation C2–The balancing market and balance settlement.

Glavan, Miha, Gradišar, Dejan, Humar, Iztok, & Vrančić, Damir (2018). Refrigeration control algorithm for managing supermarket's overall peak power demand. *IEEE Transactions on Control Systems Technology*.

Goli, Sasank, McKane, Aimee, & Olsen, Daniel (2011). *Demand response opportunities in industrial refrigerated warehouses in california: Technical report*, Berkeley, CA (United States): Lawrence Berkeley National Lab.(LBNL).

Heerup, C., & Green, T. (2014). Load shifting by ice storage in retail CO2 systems. In *11th IIR Gustav Lorentzen conference on natural refrigerants, Hangzhou, China*.

Hovgaard, Tobias Gybel, Larsen, Lars F. S., Edlund, Kristian, & Jørgensen, John Bagterp (2012). Model predictive control technologies for efficient and flexible power consumption in refrigeration systems. *Energy*, *44*(1), 105–116.

Hovgaard, Tobias Gybel, Larsen, Lars F. S., & Jørgensen, John Bagterp (2011). Flexible and cost efficient power consumption using economic MPC a supermarket refrigeration benchmark. In *2011 50th IEEE conference on decision and control and European control conference* (pp. 848–854). IEEE.

Hovgaard, Tobias Gybel, Larsen, Lars F. S., Skovrup, Morten J., & Jørgensen, John Bagterp (2011). Power consumption in refrigeration systems-modeling for optimization. In *2011 international symposium on advanced control of industrial processes (ADCONIP)* (pp. 234–239). IEEE.

Jazwinski, Andrew H. (1970). *Stochastic processes and filtering theory*. San Diego, CA, USA: Academic Press.

Juhl, Rune, Møller, Jan Kloppenborg, & Madsen, Henrik (2016). Parameter estimation in stochastic grey-box models. arXiv.

Junker, Rune Grønborg, Azar, Armin Ghasem, Lopes, Rui Amaral, Lindberg, Karen Byskov, Reynders, Glenn, Relan, Rishi, et al. (2018). Characterizing the energy flexibility of buildings and districts. *Applied Energy*, *225*, 175–182.

Kristensen, Niels Rode, Madsen, Henrik, & Jørgensen, Sten Bay (2004). Parameter estimation in stochastic grey-box models. *Automatica*, *40*(2), 225–237.

Larsen, Lars F. S., Thybo, Claus, & Rasmussen, Henrik (2007). Potential energy savings optimizing the daily operation of refrigeration systems. In *2007 European control conference (ECC)* (pp. 4759–4764). IEEE.

Murphy, M. D., O'Mahony, M. J., & Upton, J. (2015). Comparison of control systems for the optimisation of ice storage in a dynamic real time electricity pricing environment. *Applied Energy*, *149*, 392–403.

Oksendal, Bernt (2013). *Stochastic differential equations: An introduction with applications*. Springer Science & Business Media.

Parbo, Henning (2014). Balancing management with large shares of renewables. In *2nd annual European forum on grid integration and electricity anciliar services*.

Rasmussen, Lisa Buth, Bacher, Peder, Madsen, Henrik, Nielsen, Henrik Aalborg, Heerup, Christian, & Green, Torben (2016). Load forecasting of supermarket refrigeration. *Applied Energy*, *163*, 32–40.

Ueckerdt, Falko, Brecha, Robert, & Luderer, Gunnar (2015). Analyzing major challenges of wind and solar variability in power systems. *Renewable Energy*, *81*, 1–10.

Vinther, Kasper, Green, Torben, Shafiei, E., Totu, Luminita C., Izadi-Zamanabadi, Roozbeh, & Hovgaard, Tobias G. (2016). Control strategies and challenges for utilizing supermarket refrigeration systems in a smart energy context. In *2016 IEEE conference on control applications (CCA)* (pp. 593–598). IEEE.

Virtanen, Pauli, Gommers, Ralf, Oliphant, Travis E., Haberland, Matt, Reddy, Tyler, Cournapeau, David, et al. (2019). SciPy 1.0–fundamental algorithms for scientific computing in Python. arXiv preprint arXiv:1907.10121.